Nuclear matrix elements calculation for K-forbidden β-decays

R. Mancino

Institut für Kernphysik (Theoriezentrum), Fachbereich Physik, Technische Universität Darmstadt, Schlossgartenstraße 2, 64298 Darmstadt, Germany
GSI Helmholtzzentrum für Schwerionenforschung, Planckstraße 1, 64291 Darmstadt, Germany

E-mail: r.mancino@gsi.de

G. De Gregorio

Dipartimento di Matematica e Fisica, Università degli Studi della Campania "Luigi Vanvitelli", viale Abramo Lincoln 5 - I-81100 Caserta, Italy
Istituto Nazionale di Fisica Nucleare Universitario di Monte S. Angelo, Via Cintia - I-80126 Napoli, Italy

E-mail: degregorio@na.infn.it

B. Urazbekov

Institute of Nuclear Physics, 050032 Ibragimov Str. 1, Almaty, Kazakhstan
Gumilyov Eurasian National University, 010008 Satpayev Str. 2, Astana, Kazakhstan

E-mail: bakytzhan.urazbekov@gmail.com

Abstract. A certain interest in the experimental nuclear physic community has been expressed for the precise detection of the β-shape of low Q-value decays, such as ^{99}Tc $\rightarrow^{99}$ Ru$+e^{-}+\bar{\nu}_e$, tied to the search for the absolute mass of the neutrino. The necessity of a reliable way to compute the single-particle matrix elements for second forbidden operators has driven the implementation of a general algorithm to obtain the nuclear matrix elements for any given transition of generic forbiddenness K. Particular attention is then placed on the accuracy of the approximations commonly used in this context.

1. Introduction

The renewed interest in the double β-decay, stimulated by the discovery of neutrino oscillations [1, 2], reignited the interest in simple and more extreme types of β-decay to fix the problem of the quenching of the axial coupling constant g_A [3]. These extreme transitions, labelled as forbidden, are typically characterized by longer partial half-lives then the allowed decays as a consequence of the two following conditions: (1) an angular-momentum and parity change between the initial and final nuclear state is required, or (2) the transition Q value is relatively low (~ 100 keV).

These conditions are of interest to probe the absolute mass scale of neutrinos and the effective values of the weak coupling constants [4, 5]. On one hand the measurement of the electron

spectrum in β-decays can provide a direct determination of the values of neutrino masses, while on the other hand, the values of the vector coupling constant g_V and the axial-vector coupling constant g_A [6, 7] enter the β-decay theory as means of renormalizing the hadronic current.

Corrections to these bare values should account for the nuclear many-body effects that include the truncations in the model space and shortcomings in handling the many-body quantum mechanics. It is worth noting that the neutrinoless double β-decay rate is proportional to g_A^4 and for this reason the uncertainty related to the value of the axial-vector coupling constant is fundamental when considering the experimental verification of this decay.

The level of the required precision for this decay questions the validity of the usual approximations that are adopted. In particular, we have analyzed the effect of the approximations that account for the electromagnetic finite-size of the nucleus and for the deformation of the outgoing electronic wave-function [8, 9]. We have performed this study on the second forbidden non-unique β-decay of ^{99}Tc into ^{99}Ru.

This decay is of particular interest since it involves nuclei in the neighbourhood of the ^{100}Mo, one of the most promising candidates for the detection of the neutrinoless double β-decay. Moreover, recently, we have calculated the nuclear matrix element of this decay within the framework of the Realistic Shell Model [10]. The same framework, with the same inputs, is used in the current work. For this reason, the present analysis represents an important test.

2. Theory of forbidden β-decays

To approach the treatment of forbidden β-decays it is appropriate to start from the definition of the emission probability of an electron in an infinitesimal energy interval $[W_e, W_e + dW_e]$. This probability defines the shape of the β-decay spectrum and is given by

$$P(W_e) = \frac{G_F^2}{(\hbar c)^2}\frac{1}{2\pi^3\hbar}C(W_e)p_e c W_e(W_0 - W_e)F(Z, W_e), \tag{1}$$

where G_F is the Fermi coupling constant, p_e is the electron momentum and W_0 is the endpoint energy, i.e. the maximum electron energy in a given transition and the function $C(w_e)$ is the nuclear shape function that contains the information coming from the nuclear matrix elements (NMEs). The function $F(Z, W_e)$ is the Fermi function, and it takes into account the effects of the Coulomb interaction between the electron and the daughter nucleus. To obtain the decay rate for the corresponding process it is useful to define the following constant

$$\kappa = \frac{2\pi\hbar \ln(2)}{(m_e c^2)^5 (G_F cos\theta_C)^2 (\hbar c)^{-6}} = 6147\, s, \tag{2}$$

where m_e is the electron mass and θ_C is Cabibbo angle.
The measure of the half-life is given by the quantity $f_0 t_{1/2}$ called ft-value that for an allowed β-decay is given by

$$ft = \frac{\kappa}{B(a)} \quad \text{with} \quad a = F, GT, \tag{3}$$

where

$$f_0 = \int_1^{w_0} p w_e (w_0 - w_e) F(Z, w_e). \tag{4}$$

However in the case of forbidden decays the nuclear shape function $C(W_e)$ depends explicitly on the total energy of the electron W_e. Therefore it is useful to introduce an averaged nuclear shape factor so that the partial half-life $t_{1/2}$ can be obtained as $t_{1/2} = \kappa/\overline{C}$.

$$\overline{C} = \frac{1}{f_0}\int_1^{w_0} C(w_e) p w_e (w_0 - w_e) F(Z, w_e), \tag{5}$$

where the previous expressions uses the adimensional quantities $w_0 = W_0/m_e c^2$, $w_e = W_e/m_e c^2$ and $p = p_e/m_e c^2 = \sqrt{w_e^2 - 1}$. The Fermi function has been factorised as $F(Z, w_e) = F_0(Z, w_e) L_0(Z, w_e)$ to account for the electromagnetic finite-size effect where

$$L_0(Z, W_e) = \frac{1+\gamma_1}{2}\left(1 - \alpha Z W_e R + \frac{7}{15}\alpha^2 Z^2 - \frac{\gamma_1 \alpha Z R}{2W_e}\right) \tag{6}$$

where $\gamma_1 = \sqrt{1-(\alpha Z)^2}$, α is the fine structure constant and R is the nuclear charge radius of the daughter nucleus.

The information about the nuclear structure is contained in the shape factor $C(w_e)$ that consist of following combination of the NMEs

$$C(w_e) = \sum_{k_e, k_\nu, K} \lambda_{k_e}\left[M_K^2(k_e, k_\nu) + m_K^2(k_e, k_\nu) - \frac{2\gamma_{k_e}}{k_e w_e} M_K(k_e, k_\nu) m_K(k_e, k_\nu)\right]. \tag{7}$$

Here the indices k_e and k_ν come from the partial-wave expansion of respectively the electron and neutrino and within a given order of forbiddeness K leading contributions respect the relation $k_e + k_\nu = K+1$ or $k_e + k_\nu = K+2$ depending on the angular momentum transfer. Furthermore we introduced the quantity $\gamma_{k_e} = \sqrt{k_e^2 - (\alpha Z)^2}$ and the Coulomb function λ_{k_e}, whose approximated expression is

$$\lambda_{k_e} = \frac{F_{k_e - 1}(Z, W_e)}{F_0(Z, W_e)}. \tag{8}$$

The generalized Fermi function that appear in the previous expression is defined as

$$F_{k_e-1}(Z, W_e) = 4^{k_e - 1}(2k_e)(k_e + \gamma_{k_e})[(2k_e - 1)!!]^2 e^{\pi y}\left(\frac{2p_e R}{\hbar}\right)^{2(\gamma_{k_e} - k_e)}\left(\frac{|\Gamma(\gamma_{k_e} + iy)|}{\Gamma(1 + 2\gamma_{k_e})}\right)^2, \tag{9}$$

where $y = \alpha Z w_e/p$. The nuclear momenta $M_K(k_e, k_\nu)$ and $m_K(k_e, k_\nu)$ that appear in the shape factor are evaluated in the formalism of Behrens and Bühring [11, 12] using the leading-order contributions from the form-factor coefficients $\mathcal{M}^{(N)}_{KLS}(k_e, m, n, \rho)$, by assuming impulse approximation, whose explicit expression can be found in the appendix.

The form-factors $\mathcal{M}^{(N)}_{KLS}(k_e, m, n, \rho)$ contain the NMEs with the information on the nuclear structure, and for the above equations, are given by the general form

$${}^{V/A}\mathcal{M}^{(N)}_{KLS}(pn)(k_e, m, n, \rho) = \frac{\sqrt{4\pi}}{\hat{J}_i}\sum_{pn}^{V/A} m^{(N)}_{KLS}(pn)(k_e, m, n, \rho)\langle \psi_f || [c_p^\dagger \tilde{c}_n]_K || \psi_i \rangle, \tag{10}$$

where $m^{(N)}_{KLS}(pn)(k_e, m, n, \rho)$ denotes the single-particle matrix element of the K forbidden decay operators [13, 14] and $\langle \psi_f || [c_p^\dagger \tilde{c}_n]_K || \psi_i \rangle$ is the necessary one-body transition density (OBTD) that has been computed within the framework of the large scale shell model.

3. Single-particle matrix elements

The single-particle matrix elements of Eq. 10 are generated by the expectation value of the β-decay transition operators between the initial (neutron) and final (proton) single-particle wave functions, that is,

$$\begin{aligned} {}^{V}m^{(N)}_{KLS}(pn)(k_e,m,n,\rho) &= \frac{1}{\hat{K}}\langle p||T_{KLS}\big(\frac{r}{R}\big)^{2N}\mathcal{I}(k_e,m,n,\rho,r)||n\rangle \\ {}^{A}m^{(N)}_{KLS}(pn)(k_e,m,n,\rho) &= \frac{1}{\hat{K}}\langle p||\gamma_5 T_{KLS}\big(\frac{r}{R}\big)^{2N}\mathcal{I}(k_e,m,n,\rho,r)||n\rangle \end{aligned} \tag{11}$$

where

$$T_{KLS} = \begin{cases} i^L r^L Y_{LM}\delta_{LK} & S=0 \\ i^L(-1)^{L+1-K} r^L [Y_L\sigma]_{KM} & S=1 \end{cases} \tag{12}$$

and where the functions Y_{LM} are the spherical harmonics.

To compute the single-particle matrix elements the description of the single-particle initial and final states of Eq. 11 has to take into account by the relativistic single-particle spinor wave functions

$$\Phi_{nljm} = \begin{pmatrix} g_{nljm}(r) \\ f_{nljm}(r) \end{pmatrix} \tag{13}$$

where g_{nljm} is the large component of the solution of the nonrelativistic Schrödinger equation for a harmonic oscillator

$$g_{nljm}(r) = i^L g_{nl}(r)[Y_l\chi_{1/2}]_{jm} \tag{14}$$

while the small component f_{nljm} is

$$f_{nljm}(r) = \frac{\sigma\cdot p}{2M_N c} g_{nljm}(r). \tag{15}$$

In the present work for the shell model calculations we use an harmonic oscillator basis where the single-particle radial wave functions are given in terms of the oscillator parameter b by

$$g_{nl}(r) = \sqrt{\frac{2n!}{b^3\Gamma(n+l+\frac{3}{2})}}\left(\frac{r}{b}\right)^l \exp(-r^2/2b^2) L_n^{l+\frac{1}{2}}(r^2/b^2) \tag{16}$$

$$f_{nl}(r) = \frac{1}{2}\left[\left(\frac{1+n+l}{r}+\frac{r}{b^2}\right)g_{nl}(r) - \frac{2}{b}\sqrt{n+l+\frac{3}{2}}\,g_{nl+1}(r)\right]. \tag{17}$$

The explicit expressions for the single-particle matrix elements that compose the NMEs can be found in the appendix.

4. ^{99}Tc second forbidden β-decay

The second forbidden non-unique decay of $^{99}\mathrm{Tc}(9/2^+_1) \rightarrow ^{99}\mathrm{Ru}(5/2^+_1) + e^- + \bar{\nu_e}$ poses an interesting challenge as the relatively small Q-window of the reaction, that is the range of energies that the produced electron can assume, stresses the need of reliable calculation at particularly low momenta of the e^-. In turn this translate into the need of an accurate description of the electronic wave-function and in particular the set of Coulomb functions λ_k (Eq. 8) for $k = 2, 3$. The values of λ_2 and λ_3 obtained trough the approximated expression for λ_k (Eq. 8) are in very good agreement with the values tabulated by Behrens and Jänecke [15] obtained solving the Dirac equation for the electron wave-function.

Table 1. Comparison of the $\log(ft)$ values in the $L_0 = 1$, $\lambda_k = 1$ approximation and when no such approximation is used.

Approx.	$log(ft)$
$L_0 = 1$	12.59
$\lambda_k = 1$	13.17
No approx.	12.58

Regarding the evaluation of the NMEs, in this work, the OBTD were computed adopting the nuclear shell model code KSHELL [16]. We have considered a valence space that is spanned by the $0f_{5/2}$, $1p_{3/2}$, $1p_{1/2}$, $0g_{9/2}$ proton and $0g_{7/2}$, $1d_{5/2}$, $1d_{3/2}$, $2s_{1/2}$ neutron orbitals, also used in previous works (Ref. [10]).

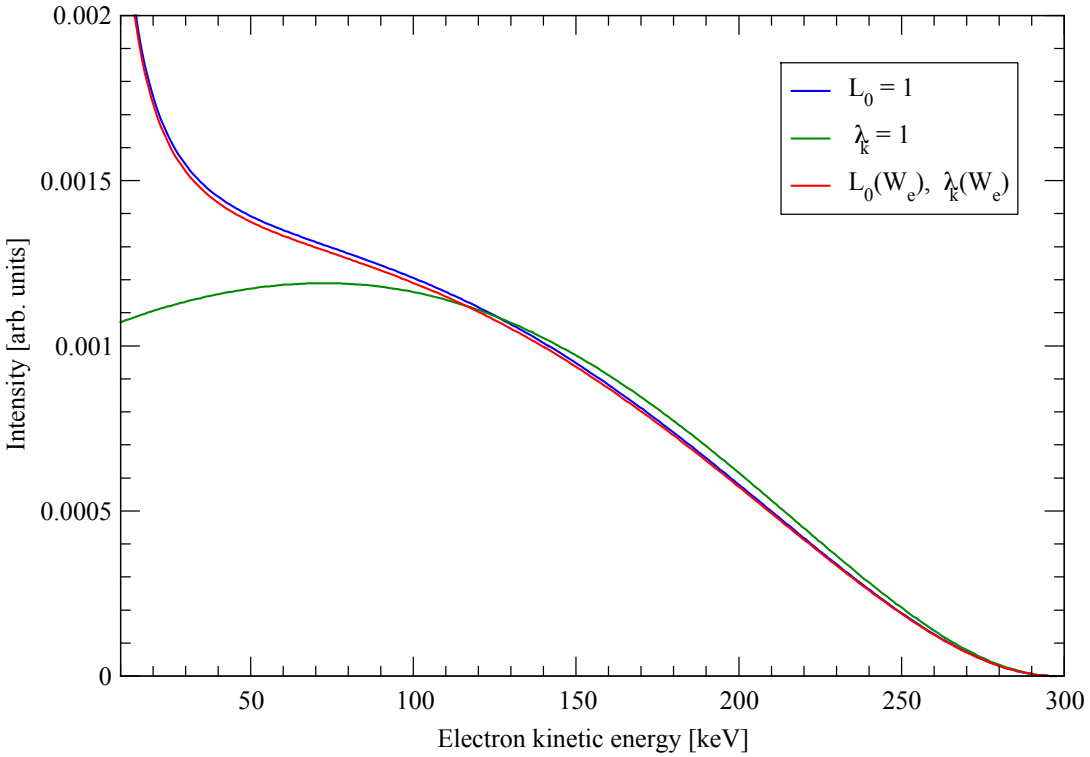

Figure 1. Comparison of the β-spectrum in the $L_0 = 1$, $\lambda_k = 1$ approximation and when such approximation is not used. To perform the comparison between the three, the areas under each curve are normalized to the respective ft-value.

The two body effective interaction was obtained within the framework of the many-body perturbation theory starting from the CD-Bonn nucleon-nucleon potential [17] that has been renormalized via V_{low-k} procedure [18]. In this work the value of the axial-vector coupling constant adopted is $g_A = 1.27$.

From the comparison in Fig. 1 and the values of the $\log(ft)$ shown in Tab. 1 it is apparent that the commonly used $\lambda_k = 1$ approximation doesn't provide a good description. While the correction for the electromagnetic finite-size of the nucleus given by the function L_0 plays a negligible role, it is necessary to not resort to the $\lambda_k = 1$ approximation for the Coulomb function, especially for low momenta of the electron. This was expected since the $\lambda_k = 1$ approximation [19] requires $\gamma_{k_e} - k_e \sim O\{(\alpha Z)^2\}$ to vanish faster than $y = \alpha Z w_e/p \sim O(\alpha Z)$ for $\alpha Z \to 0$. However, in this case, since $Z = 44$ and $w_e \to 0$, this condition is not satisfied.

The experimental measurement of the β-decay $\log(ft)$ of the $^{99}\mathrm{Tc}(9/2^+_1)$ to the $^{99}\mathrm{Ru}(5/2^+_1)$ was performed in Ref. ([20]). The experimental result was $\log(ft) = 12.33$.

In the case of a shell-model calculation the operators are defined in a restricted space model and the excluded degrees of freedom are taken into account defining an effective axial-vector coupling constant. This is produced via the introduction of a normalization factor such that $g_A^{\mathrm{eff}} = q\, g_A$. Usually, for a β-decay operator $q < 1$ [21, 22], therefore one refers to it as quenching factor. In this case, to reproduce the experimental value, a very unorthodox normalization factor ($q = 1.33$) is required.

From this we can draw only two possible conclusions: (1) as Engelke and Ullman observe in their work, it is possible that contaminations in the sample lead to an underestimation of the half-life of $^{99}\mathrm{Tc}(9/2^+)$ and more precise measurements are required or (2) an evaluation on the quenching factor must be carried out individually on each operator that drives this second forbidden decay. The second possibility arises from the fact that the nuclear shape factor $C(w_e)$ is a non-linear combination of all the possible second forbidden decay operators. For this reason, a mere global quenching of the axial-vector coupling constant cannot take into account eventual cancellation or interference terms between these operators. To preserve the predictive power of the shell-model, however, a framework in which the quenching of the operators arises naturally from a perturbation theory approach is required, such as the Realistic Shell Model [23], that offers a microscopic description of the nucleus without resorting to empirical adjustments.

Acknowledgements
We acknowledge ACRI - organisation of Foundations of banking origin and Savings Banks - for the financial support provided for the participation in the conference from the grant "YOUNG INVESTIGATOR TRAINING PROGRAM 2019" as well as the SFB 1245 - Nuclei: From Fundamental Interactions to Structure and Stars - project founded by the Deutsche Forschungsgemeinschaft (DFG). This work is co-funded by EU-FESR, PON Ricerca e Innovazione 2014-2020 - DM 1062/2021.

Appendix A
In the case of $k_e + k_\nu = K + 1$, $M_K(k_e, k_\nu)$ and $m_K(k_e, k_\nu)$ are given by

$$
\begin{aligned}
M_K(k_e,k_\nu) &= \mathcal{K}_K \xi^{k_e+k_\nu} (\sqrt{w_e^2-1})^{k_e-1} (w_0-w_e)^{k_\nu-1} \Bigg[\sqrt{\frac{2K+1}{K}} R^{-(K-1)} g_V^V \mathcal{M}^{(0)}_{KK-11} \\
&- \left(\frac{w_e}{2k_e+1} + \frac{w_0-w_e}{2k_\nu+1} \right) \xi R^{-K} g_V^V \mathcal{M}^{(0)}_{KK0} - \frac{\alpha Z}{2k_e+1} R^{-K} g_V^V \mathcal{M}^{(0)}_{KK0}(k_e,1,1,1) \\
&+ \sqrt{\frac{K+1}{K}} \left(\frac{w_e}{2k_e+1} - \frac{w_0-w_e}{2k_\nu+1} \right) \xi R^{-K} g_A^A \mathcal{M}^{(0)}_{KK1} + \sqrt{\frac{K+1}{K}} \frac{\alpha Z}{2k_e+1} R^{-K} g_A^A \mathcal{M}^{(0)}_{KK1}(k_e,1,1,1)
\end{aligned}
$$

$$
\begin{aligned}
&- 2\sqrt{\frac{K+1}{2K+1}}\frac{w_e}{2k_e+1}\frac{w_0-w_e}{2k_\nu+1}\xi^2 R^{-(K+1)} g_V^V \mathcal{M}^{(0)}_{KK+11} \\
&- 2\sqrt{\frac{K+1}{2K+1}}\frac{\alpha Z}{2k_e+1}\frac{w_0-w_e}{2k_\nu+1}\xi^2 R^{-(K+1)} g_V^V \mathcal{M}^{(0)}_{KK+11}(k_e,1,1,1) \\
&+ \frac{1}{\sqrt{K(2K+1)}}\frac{w_e}{2k_e+1}\frac{w_0-w_e}{2k_\nu+1}\xi^2 R^{-(K-1)} g_V^V \mathcal{M}^{(1)}_{KK-11} \\
&+ \frac{1}{2}\sqrt{\frac{2K+1}{K}}\left(\frac{1}{2k_e+1}-\frac{w_e^2}{2k_e+1}-\frac{(w_0-w_e)^2}{2k_\nu+1}\right)\xi^2 R^{-(K-1)} g_V^V \mathcal{M}^{(1)}_{KK-11} \\
&+ \frac{1}{\sqrt{K(2K+1)}}\frac{\alpha Z}{2k_e+1}\frac{w_0-w_e}{2k_\nu+1}\xi R^{-(K-1)} g_V^V \mathcal{M}^{(1)}_{KK-11}(k_e,1,1,1) \\
&- \sqrt{\frac{2K+1}{K}}\frac{\alpha Z w_e}{2k_e+1}\xi R^{-(K-1)} g_V^V \mathcal{M}^{(1)}_{KK-11}(k_e,2,2,1) \\
&- \frac{1}{2}\sqrt{\frac{2K+1}{K}}\frac{(\alpha Z)^2}{2k_e+1} R^{-(K-1)} g_V^V \mathcal{M}^{(1)}_{KK-11}(k_e,2,2,2)\Bigg]
\end{aligned}
\tag{18}
$$

$$
\begin{aligned}
m_K(k_e,k_\nu) &= \mathcal{K}_K \xi^{k_e+k_\nu-1}(\sqrt{w_e^2-1})^{k_e-1}(w_0-w_e)^{k_\nu-1}\frac{1}{2k_e+1}\Bigg[-R^{-K} g_V^V \mathcal{M}^{(0)}_{KK0} \\
&+ \sqrt{\frac{K+1}{K}} R^{-K} g_A^A \mathcal{M}^{(0)}_{KK1} - 2\sqrt{\frac{K+1}{2K+1}}\frac{w_0-w_e}{2k_\nu+1}\xi R^{-(K+1)} g_V^V \mathcal{M}^{(0)}_{KK1} \\
&+ \frac{1}{\sqrt{K(2K+1)}}\frac{w_0-w_e}{2k_\nu+1}\xi R^{-K-1} g_V^V \mathcal{M}^{(1)}_{KK-11} - \frac{1}{2}\sqrt{\frac{2K+1}{K}}\alpha Z R^{-(K-1)} g_V^V \mathcal{M}^{(1)}_{KK-11}(k_e,2,1,1)\Bigg]
\end{aligned}
\tag{19}
$$

Where we have introduced the quantity $\xi = m_e c^2 R/(\hbar c)$ and

$$
\mathcal{K}_K = \sqrt{\frac{1}{2}}\sqrt{\frac{(2K)!!}{(2K+1)!!}}\sqrt{\frac{1}{(2k_e-1)!(2k_\nu-1)!}} \tag{20}
$$

In the case of $k_e + k_\nu = K + 2$ instead

$$
\begin{aligned}
M_K(k_e,k_\nu) &= \tilde{\mathcal{K}}_K \xi^{k_e+k_\nu-2}(\sqrt{w_e^2-1})^{k_e-1}(w_0-w_e)^{k_\nu-1}\sqrt{\frac{K+1}{(2k_e-1)(2k_\nu-1)}}\Bigg[R^{-(K)} g_V^V \mathcal{M}^{(0)}_{KK0} \\
&+ \frac{k_e-k_\nu}{\sqrt{K(K+1)}} R^{-K} g_A^A \mathcal{M}^{(0)}_{KK1} + \sqrt{\frac{1}{(K+1)(2K+1)}}\left(\frac{2k_e-1}{2k_e+1}w_e + \frac{2k_\nu-1}{2k_\nu+1}(w_0-w_e)\right)\xi R^{-(K+1)} g_V^V \mathcal{M}^{(0)}_{KK+11} \\
&+ \sqrt{\frac{1}{(K+1)(2K+1)}}\frac{2k_e-1}{2k_e+1}\alpha Z R^{-(K+1)} g_V^V \mathcal{M}^{(0)}_{KK+11}(k_e,1,1,1) \\
&+ \sqrt{\frac{1}{(K+1)(2K+1)}}\left(\frac{2(k_e-1)}{2k_e+1}w_e + \frac{2(k_e-1)}{2k_\nu+1}(w_0-w_e)\right)\xi R^{-(K-1)} g_V^V \mathcal{M}^{(1)}_{KK-11} \\
&+ \sqrt{\frac{1}{K(2K+1)}}\frac{2(k_\nu-1)}{2k_e+1}\alpha Z R^{-(K-1)} g_V^V \mathcal{M}^{(1)}_{KK-11}(k_e,1,1,1)\Bigg]
\end{aligned}
\tag{21}
$$

$$m_K(k_e,k_\nu)=\tilde{\mathcal{K}}_K\xi^{k_e+k_\nu-1}(\sqrt{w_e^2-1})^{k_e-1}(w_0-w_e)^{k_\nu-1}\sqrt{\frac{K+1}{(2k_e+1)(2k_\nu+1)}}\frac{1}{2k_e+1}$$
$$\left[\sqrt{\frac{1}{(K+1)(2K+1)}}(2k_e-1)R^{-(K+1)}g_V^V\mathcal{M}^{(0)}_{KK+11}+2\sqrt{\frac{1}{K(2K+1)}}(k_\nu-1)R^{-K}g_A^A\mathcal{M}^{(1)}_{KK1}\right] \tag{22}$$

where the factor $\mathcal{K}_K$ changes to

$$\tilde{\mathcal{K}}_K=\sqrt{\frac{(2K)!!}{(2K+1)!!}}\sqrt{\frac{1}{(2k_e-1)!(2k_\nu-1)!}}\nu \tag{23}$$

Additionally the following terms have to be evaluated

$$\begin{aligned}M_{K+1}(k_e,k_\nu)=\tilde{\mathcal{K}}_K\xi^{k_e+k_\nu-2}(\sqrt{w_e^2-1})^{k_e-1}(w_0-w_e)^{k_\nu-1}\Bigg[&-R^{-K}g_A^A\mathcal{M}^{(0)}_{K+1K1}\\
&+\sqrt{\frac{K+1}{2K+3}}\left(\frac{w_e}{2k_e+1}+\frac{w_0-w_e}{2k_\nu+1}\right)\xi R^{-(K+1)}g_A^A\mathcal{M}^{(0)}_{K+1K+10}\\
&+\sqrt{\frac{K+1}{2K+3}}\frac{\alpha Z}{2k_e+1}R^{-(K+1)}g_A^A\mathcal{M}^{(0)}_{K+1K+10}(k_e,1,1,1)\\
&-\sqrt{\frac{K+2}{2K+3}}\left(\frac{w_e}{2k_e+1}-\frac{w_0-w_e}{2k_\nu+1}\right)\xi R^{-(K+1)}g_V^V\mathcal{M}^{(0)}_{K+1K+11}\\
&-\sqrt{\frac{K+2}{2K+3}}\frac{\alpha Z}{2k_e+1}R^{-(K+1)}g_V^V\mathcal{M}^{(0)}_{K+1K+11}(k_e,1,1,1)\Bigg]\end{aligned} \tag{24}$$

Appendix B

In the Condon-Shortley phase convention the single-particle matrix elements are given by

$$\begin{aligned}{}^{V}m^{(N)}_{KK0}(pn)(k_e,m,n,\rho)=&\sqrt{\frac{2}{2J_i+1}}\\
\Bigg[&G_{KK0}(\kappa_p,\kappa_n)\int_0^\infty g_p(r,\kappa_p)\left(\frac{r}{R}\right)^{K+2N}\mathcal{I}(k_e,m,n,\rho,r)g_n(r,k_n)r^2dr\\
&+G_{KK0}(-\kappa_p,-\kappa_n)\int_0^\infty f_p(r,\kappa_p)\left(\frac{r}{R}\right)^{K+2N}\mathcal{I}(k_e,m,n,\rho,r)f_n(r,k_n)r^2dr\Bigg]\end{aligned} \tag{25}$$

$$\begin{aligned}{}^{A}m^{(N)}_{KK0}(pn)(k_e,m,n,\rho)=&\sqrt{\frac{2}{2J_i+1}}\\
\Bigg[&G_{KK0}(\kappa_p,-\kappa_n)\int_0^\infty g_p(r,\kappa_p)\left(\frac{r}{R}\right)^{K+2N}\mathcal{I}(k_e,m,n,\rho,r)f_n(r,k_n)r^2dr\\
&-G_{KK0}(-\kappa_p,\kappa_n)\int_0^\infty f_p(r,\kappa_p)\left(\frac{r}{R}\right)^{K+2N}\mathcal{I}(k_e,m,n,\rho,r)g_n(r,k_n)r^2dr\Bigg]\end{aligned} \tag{26}$$

$$
\begin{aligned}
&{}^{V}m^{(N)}_{KL1}(pn)(k_e,m,n,\rho) = \mathrm{sign}(K-L+\frac{1}{2})\sqrt{\frac{2}{2J_i+1}} \\
&\Bigg[G_{KL1}(\kappa_p,-\kappa_n)\int_0^\infty g_p(r,\kappa_p)\left(\frac{r}{R}\right)^{L+2N}\mathcal{I}(k_e,m,n,\rho,r)f_n(r,k_n)r^2dr \\
&-G_{KK0}(-\kappa_p,\kappa_n)\int_0^\infty f_p(r,\kappa_p)\left(\frac{r}{R}\right)^{L+2N}\mathcal{I}(k_e,m,n,\rho,r)g_n(r,k_n)r^2dr\Bigg]
\end{aligned}
\tag{27}
$$

$$
\begin{aligned}
&{}^{A}m^{(N)}_{KL1}(pn)(k_e,m,n,\rho) = \mathrm{sign}(K-L+\frac{1}{2})\sqrt{\frac{2}{2J_i+1}} \\
&\Bigg[G_{KK0}(\kappa_p,\kappa_n)\int_0^\infty g_p(r,\kappa_p)\left(\frac{r}{R}\right)^{L+2N}\mathcal{I}(k_e,m,n,\rho,r)g_n(r,k_n)r^2dr \\
&+G_{KK0}(-\kappa_p,-\kappa_n)\int_0^\infty f_p(r,\kappa_p)\left(\frac{r}{R}\right)^{L+2N}\mathcal{I}(k_e,m,n,\rho,r)f_n(r,k_n)r^2dr\Bigg]
\end{aligned}
\tag{28}
$$

where the quantity $G_{KLS}(k_p,k_n)$ is given by

$$
\begin{aligned}
G_{KLS}(k_p,k_n) =&(-1)^{j_p-j_n+l_p}\hat{S}\hat{K}\hat{j}_p\hat{j}_n\hat{l}_p\hat{l}_n \\
&\langle l_p l_n 00|L0\rangle \begin{Bmatrix} K & S & L \\ j_p & \frac{1}{2} & l_p \\ j_n & \frac{1}{2} & l_n \end{Bmatrix}
\end{aligned}
\tag{29}
$$

and $\hat{S}=\sqrt{2S+1}$ is the usual hat notation.

The functions $\mathcal{I}(k_e,m,n,\rho,r)$ account for a finite nucleus with uniform charge distribution and are tabulated for different values of the parameters k_e,m,n,ρ [12].

References

[1] Y. Fukuda, T. Hayakawa, E. Ichihara, K. Inoue, K. Ishihara, H. Ishino, Y. Itow, T. Kajita, J. Kameda, S. Kasuga, K. Kobayashi, Y. Kobayashi, Y. Koshio, M. Miura, M. Nakahata, S. Nakayama, A. Okada, K. Okumura, N. Sakurai, M. Shiozawa, Y. Suzuki, Y. Takeuchi, Y. Totsuka, S. Yamada, M. Earl, A. Habig, E. Kearns, M. D. Messier, K. Scholberg, J. L. Stone, L. R. Sulak, C. W. Walter, M. Goldhaber, T. Barszczxak, D. Casper, W. Gajewski, P. G. Halverson, J. Hsu, W. R. Kropp, L. R. Price, F. Reines, M. Smy, H. W. Sobel, M. R. Vagins, K. S. Ganezer, W. E. Keig, R. W. Ellsworth, S. Tasaka, J. W. Flanagan, A. Kibayashi, J. G. Learned, S. Matsuno, V. J. Stenger, D. Takemori, T. Ishii, J. Kanzaki, T. Kobayashi, S. Mine, K. Nakamura, K. Nishikawa, Y. Oyama, A. Sakai, M. Sakuda, O. Sasaki, S. Echigo, M. Kohama, A. T. Suzuki, T. J. Haines, E. Blaufuss, B. K. Kim, R. Sanford, R. Svoboda, M. L. Chen, Z. Conner, J. A. Goodman, G. W. Sullivan, J. Hill, C. K. Jung, K. Martens, C. Mauger, C. McGrew, E. Sharkey, B. Viren, C. Yanagisawa, W. Doki, K. Miyano, H. Okazawa, C. Saji, M. Takahata, Y. Nagashima, M. Takita, T. Yamaguchi, M. Yoshida, S. B. Kim, M. Etoh, K. Fujita, A. Hasegawa, T. Hasegawa, S. Hatakeyama, T. Iwamoto, M. Koga, T. Maruyama, H. Ogawa, J. Shirai, A. Suzuki, F. Tsushima, M. Koshiba, M. Nemoto, K. Nishijima, T. Futagami, Y. Hayato, Y. Kanaya, K. Kaneyuki, Y. Watanabe, D. Kielczewska, R. A. Doyle, J. S. George, A. L. Stachyra, L. L. Wai, R. J. Wilkes, and K. K. Young. Evidence for oscillation of atmospheric neutrinos. *Phys. Rev. Lett.*, 81:1562–1567, Aug 1998.

[2] A. Bellerive, J.R. Klein, A.B. McDonald, A.J. Noble, and A.W.P. Poon. The sudbury neutrino observatory. *Nuclear Physics B*, 908:30–51, 2016. Neutrino Oscillations: Celebrating the Nobel Prize in Physics 2015.

[3] Jouni T. Suhonen. Value of the axial-vector coupling strength in β and $\beta\beta$ decays: A review. *Frontiers in Physics*, 5:55, November 2017.

[4] Frank T. Avignone, Steven R. Elliott, and Jonathan Engel. Double beta decay, majorana neutrinos, and neutrino mass. *Rev. Mod. Phys.*, 80:481–516, Apr 2008.
[5] J. D. Vergados, H. Ejiri, and F. Šimkovic. *Rep. Prog. Phys.*, 75:106301, 2012.
[6] M. Haaranen, P. C. Srivastava, and J. Suhonen. Forbidden nonunique β decays and effective values of weak coupling constants. *Phys. Rev. C*, 93:034308, Mar 2016.
[7] Joel Kostensalo and Jouni Suhonen. $g_{\rm a}$-driven shapes of electron spectra of forbidden β decays in the nuclear shell model. *Phys. Rev. C*, 96:024317, Aug 2017.
[8] X. Mougeot and C. Bisch. Consistent calculation of the screening and exchange effects in allowed β^- transitions. *Phys. Rev. A*, 90:012501, Jul 2014.
[9] X. Mougeot. Reliability of usual assumptions in the calculation of β and ν spectra. *Phys. Rev. C*, 91:055504, May 2015.
[10] L. Coraggio, N. Itaco, G. De Gregorio, A. Gargano, R. Mancino, and F. Nowacki. Shell-model calculation of ^{100}Mo double-β decay. *Phys. Rev. C*, 105:034312, Mar 2022.
[11] H. Behrens and W. Bühring. *Nucl. Phys. A*, 162:111, 1971.
[12] Heinrich Behrens and Wolfgang Bühring. *Electron radial wave functions and nuclear betadecay.* Number 67. Oxford University Press, USA, 1982.
[13] M. Haaranen, J. Kotila, and J. Suhonen. Spectrum-shape method and the next-to-leading-order terms of the β-decay shape factor. *Phys. Rev. C*, 95:024327, Feb 2017.
[14] Fahlin Strömberg Dag Isak August. Weak interactions in degenerate oxygen-neon cores. pages vi, 111 Seiten, 2020.
[15] H. Behrens and J. Janecke. *Numerical Tables for Beta-Decay and Electron Capture.* Springer, Berlin, 1969.
[16] Noritaka Shimizu, Takahiro Mizusaki, Yutaka Utsuno, and Yusuke Tsunoda. Thick-restart block lanczos method for large-scale shell-model calculations. *Computer Physics Communications*, 244:372 – 384, 2019.
[17] R. Machleidt. *Phys. Rev. C*, 63:024001, 2001.
[18] L. Coraggio, A. Covello, A. Gargano, N. Itaco, and T. T. S. Kuo. *Ann. Phys. (NY)*, 327:2125, 2012.
[19] H. Behrens and W. Bühring. *Electron Radial Wave Functions and Nuclear Beta-decay.* International series of monographs on physics. Clarendon Press, 1982.
[20] C. E. Engelke and J. D. Ullman. Observation of a weak beta-decay branch in ^{99}Tc. *Phys. Rev. C*, 9:2358–2362, Jun 1974.
[21] L. Coraggio, L. De Angelis, T. Fukui, A. Gargano, N. Itaco, and F. Nowacki. Renormalization of the gamow-teller operator within the realistic shell model. *Phys. Rev. C*, 100:014316, Jul 2019.
[22] B. Alex Brown and K. Rykaczewski. Gamow-teller strength in the region of ^{100}Sn. *Phys. Rev. C*, 50:R2270–R2273, Nov 1994.
[23] L. Coraggio, A. Covello, A. Gargano, N. Itaco, and T. T. S. Kuo. *Prog. Part. Nucl. Phys.*, 62:135, 2009.